

# Miscibility, density and viscosity of poly(dimethylsiloxane) in supercritical carbon dioxide

Yan Xiong and Erdogan Kiran\*

Department of Chemical Engineering, University of Maine, Orono, ME 04469-5737, USA  
(Received 2 March 1995; revised 5 May 1995)

Phase boundaries, densities and viscosities of solutions of poly(dimethylsiloxane)s (PDMS) in supercritical carbon dioxide have been determined. The demixing pressures of 5 wt% solutions of PDMS of different molecular weights ( $M_w = 38\,900$ ,  $M_w/M_n = 2.84$ ;  $M_w = 93\,700$ ,  $M_w/M_n = 2.99$ ;  $M_w = 273\,500$ ,  $M_w/M_n = 2.29$ ;  $M_w = 369\,200$ ,  $M_w/M_n = 2.19$ ) were determined in the temperature range from 300 to 460 K. At temperatures above 330 K the solutions show typical lower critical solution temperature behaviour and the demixing pressures increase with temperature. Below 330 K, the behaviour is reversed, and demixing pressures show a dramatic increase with decreasing temperature. The phase boundaries and the steep changes in the demixing pressures with temperature are discussed in the framework of the Sanchez–Lacombe model. Evaluation of the demixing pressures along with information on the details of molecular weight distributions obtained by gel permeation chromatography show that the observed demixing pressures are very much influenced by the high-molecular-weight tails of the distributions. Analysis of the density and viscosity data for solutions of PDMS with  $M_w = 38\,900$  at 1, 2 and 5 wt% concentrations show that results can be correlated with a free-volume based relationship of the form  $\eta = A \exp[B/(1 - C\rho)]$ . Analysis of the pressure dependence of viscosity at selected temperatures shows that the apparent activation volumes are in the range of 30 to 60 cm<sup>3</sup> mol<sup>-1</sup>. Analysis of the temperature dependence at different pressures gives activation energies in the range 7–10 kJ mol<sup>-1</sup>.

(Keywords: poly(dimethylsiloxane); supercritical carbon dioxide; modelling)

## INTRODUCTION

The use of supercritical fluids in polymer formation, modification and processing has been discussed in detail in a recent review article<sup>1</sup>. There are many reasons for the growing interest in these fluids for polymer applications. The replacement of conventional organic solvents with environmentally less harmful fluids such as carbon dioxide is a major motivation. In addition, introduction of a supercritical fluid component introduces pressure and/or the solvent composition as adjustable parameters for better control of a given process. Specific examples include: (1) controlling the miscibility conditions to regulate molecular weight and molecular weight distributions during polymerization; (2) controlling the swelling of polymer matrices, along with controlled diffusivity, viscosity and phase separation conditions, to regulate impregnations; (3) controlling solubility to bring about selective extractions, fractionations or separations; and (4) controlling viscosity to regulate the rheological properties of polymer melts or solutions at the final processing stage.

Although thermodynamic aspects such as the influence of pressure, temperature and the fluid type on the miscibility of polymers in supercritical fluids have been studied to some extent, information on transport

properties such as the viscosities of polymer solutions in supercritical fluids is rather limited. Experimental data and predictive models on the viscosity of polymer solutions at high pressures are crucial for a number of applications ranging from lubrication<sup>2</sup> to enhanced oil recovery<sup>3</sup>, and to supercritical processing<sup>1,4–6</sup>. In polymer processing, viscosity is a key factor influencing general operations such as pumping, mixing and mass and heat transfer, and more specific aspects such as spinnability (for fibre formation), spray characteristics and droplet formation (for coatings or particle formations) and penetration (in composites manufacture). Recent reviews<sup>4,7</sup> show that there are essentially no high-pressure viscosity data for polymer solutions prior to 1979, and that most of the available information, even though covering high pressures, is limited to subcritical temperatures.

We have already reported on the viscosity of solutions of polystyrene and polyethylene as a function of molecular weight and concentration in near-critical and supercritical alkanes<sup>1,4,7</sup>. In the present paper, we report on the viscosity of solutions of poly(dimethylsiloxane)s (PDMS) in supercritical carbon dioxide at a polymer concentration of 5 wt% in the temperature range from 380 to 400 K and pressures up to 70 MPa.

Unlike polystyrene and polyethylene, PDMS is a liquid at room temperature and is highly soluble in supercritical carbon dioxide at high pressures. One of the earliest

\*To whom correspondence should be addressed

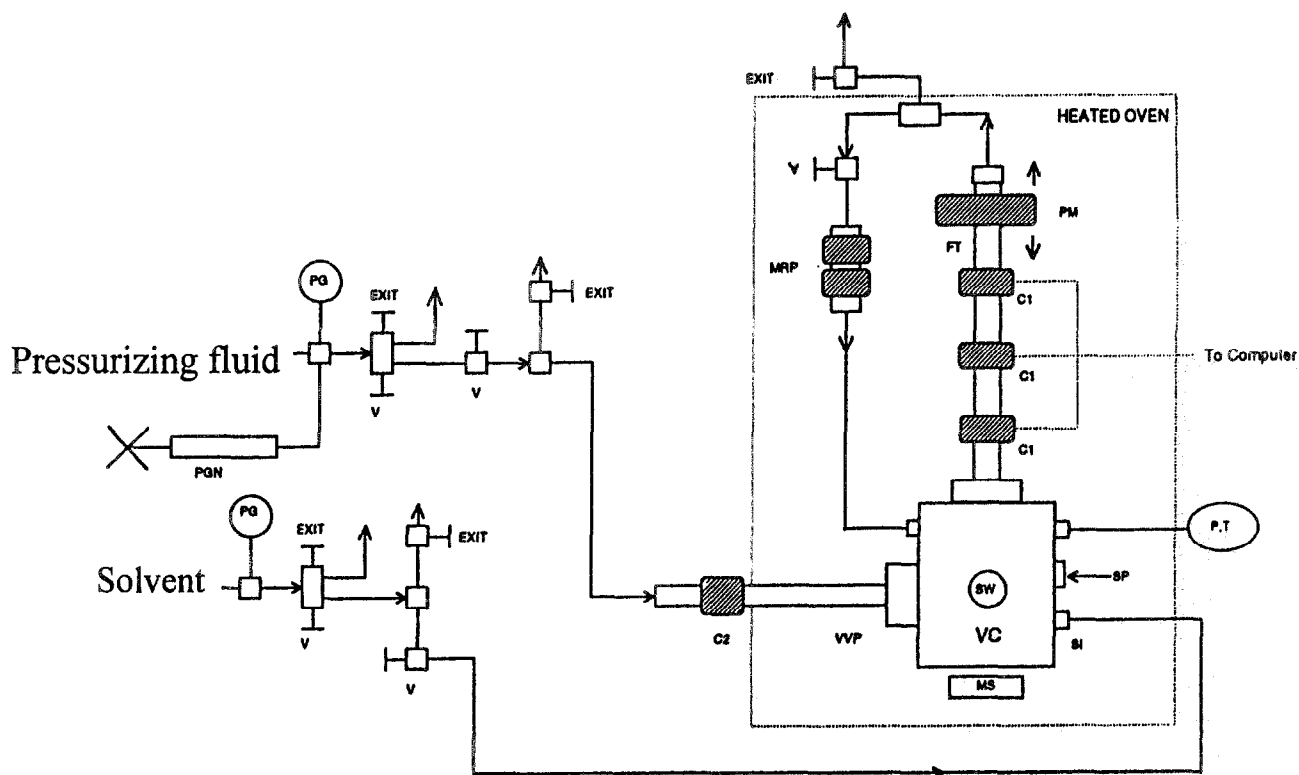


**Figure 1** Experimental system for measurement of viscosity and density (VVP = variable volume piston; VC = view cell; SW = sapphire window; MS = magnetic stirrer; SI = solvent inlet; SP = solute loading port; P, T = pressure and temperature sensor; FT = fall tube; PM = pull-up magnet; MRP = magnetic recirculation pump; V = valve; C1, C2 = LVDT coils; PGN = pressure generator; PG = pressure gauge)

reports on the solubility of poly(dimethylsiloxane)s in carbon dioxide was in connection with explorations related to direct thickeners for mobility control of carbon dioxide floods in enhanced oil recovery<sup>3</sup>. It was reported that at 25°C and 18 MPa, the solubility of a PDMS sample ( $M_w = 135\,000$ ) in CO<sub>2</sub> was 0.3 g l<sup>-1</sup>; this increased to ~1.0 g l<sup>-1</sup> at 52°C. Supercritical carbon dioxide has also been used to fractionate poly(dimethylsiloxane)s<sup>8,9</sup>. It has been explored for purification of liquid-crystalline siloxane oligomers<sup>10</sup> at 80°C and at pressures in the range from 14 to 31 MPa. More recent studies are exploring the reduction of viscosity of PDMS upon addition of supercritical carbon dioxide<sup>5,6,11</sup>. Specifically, solubility of supercritical CO<sub>2</sub> in PDMS melts has been reported in the temperature range 50–100°C at pressures up to 26 MPa (ref. 11). At 50°C and 26 MPa, carbon dioxide solubility in PDMS is reported to be ~40 wt%. At higher temperatures the solubility is reduced to ~20 wt% at 26 MPa at 100°C. Volumetric and viscometric behaviour of carbon dioxide/PDMS mixtures at high PDMS concentrations have been reported<sup>5,6</sup> in the temperature range 30–70°C and the pressure range 10–70 MPa. A major consequence of adding carbon dioxide to the polymer melts is to decrease their viscosity. Clearly, reduction of polymer melt viscosity is of great importance to extrusion and foaming, as well as impregnation processes for composites manufacturing. Our interest in the current study is in the other extreme, where the presence of the polymer increases the viscosity of the solvent.

The present viscosity data have been generated using a special viscometer<sup>7,12,13</sup> which also provides information on the phase boundaries and the densities of the solutions.

As a result, thermodynamic and transport properties are studied in the same instrument for the same solutions. Using the information on the phase-state of the solutions, the density and viscosity measurements are conducted at conditions corresponding to homogeneous one-phase regions.

Our previous studies<sup>14–17</sup> have shown that lattice models such as the Sanchez–Lacombe model or the statistical associating fluid theory (SAFT) can be used to predict the phase boundaries. In the present study, we have used the Sanchez–Lacombe formalism to model the pressure–volume–temperature (*PVT*) behaviour and the phase boundaries. Data on demixing pressures have been also analysed and compared with respect to molecular weight and molecular weight distribution of the polymer, polymer concentration and the temperature.

Viscosity data have been analysed with respect to their dependence on temperature (at constant pressure) and pressure (at constant temperature), from which information on the flow activation energies and the activation volumes are evaluated. The variation of viscosity with density has also been documented and the effectiveness of free-volume concepts in describing the viscosity of the solutions have been demonstrated.

## EXPERIMENTAL

### Materials

The poly(dimethylsiloxane) samples with weight-average molecular weights  $M_w = 38\,900$  ( $M_w/M_n = 2.84$ ), 93 700 ( $M_w/M_n = 2.99$ ) and 369 200 ( $M_w/M_n = 2.19$ ) were obtained from Scientific Polymer Products, and a sample with  $M_w = 273\,500$  ( $M_w/M_n = 2.29$ ) was

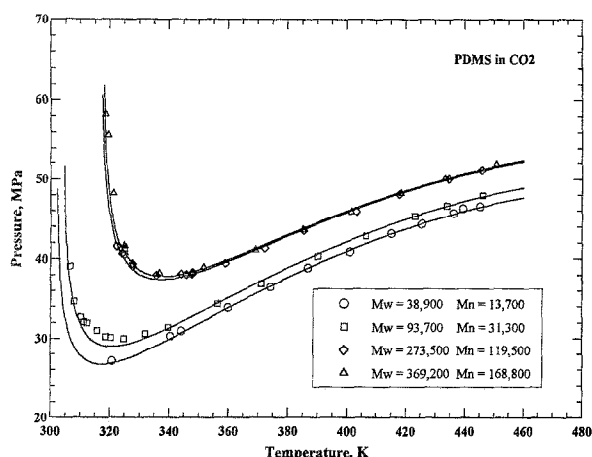


**Figure 2** Demixing pressures for poly(dimethylsiloxane) solutions (5 wt%) in supercritical carbon dioxide. Solid curves are predictions by the Sanchez-Lacombe model

obtained from Aldrich. Carbon dioxide (purity > 99.9%) was obtained from Liquid Carbonic and used without further purification.

#### Determination of density, viscosity and demixing pressures

Figure 1 is a schematic diagram of the experimental system used to measure density and viscosity and to assess the phase-state of the solutions. Details of this system have been given in our earlier publications<sup>12,13</sup>. Briefly, it consists of a variable-volume view cell (VC), a fall tube (FT) and a circulation loop which are all housed in a heated oven. After loading the cell with the polymer and the solvent fluid, at a given temperature, the pressure is increased until homogeneous one-phase conditions are obtained. The dissolution process is facilitated with the mixing action of a magnetic stirring bar placed in the view cell, and by the recirculation of the cell contents with a magnetic pump (MRP). Once the cell is loaded, the pressure changes are brought about with a pressure generator (PGN) through movement of a piston inside the variable-volume part (VVP) of the view cell. A linear variable differential transformer (LVDT) coil monitors the position of the piston and hence provides information on the internal volume of the system at any temperature and pressure. From the knowledge of the initial mass of solution loaded into the cell, and the volume as calculated from the piston position, densities are calculated directly. Viscosity determinations are based on the measurement of the fall time of a cylindrical sinker in the fall tube. Three LVDT coils are used to monitor the movement of the sinker, from which fall times are calculated. Viscosity is then determined from a relationship of the form  $\eta = K(\rho_s - \rho)t$ , where  $K$  is a calibration constant,  $\rho_s$  and  $\rho$  are the densities of the sinker and fluid, respectively, and  $t$  is the fall time of the sinker. The calibration constant is determined by measuring the viscosities of fluids of known viscosity over a wide range of pressures and temperatures. The procedure for calibration involves corrections for both temperature and pressure<sup>7,12,13</sup>. Using this system, densities and viscosities are determined in general with an accuracy of  $\pm 1\%$  and  $3\%$ , respectively, at pressures up to 70 MPa and temperatures up to 200°C.

To eliminate any ambiguity which may arise from inaccessibility of the solution in the fall tube to visual observation, demixing pressures were further verified by independent measurements in a standard variable-volume view cell that we routinely use for investigation of the phase behaviour of polymer/solvent systems<sup>14,15</sup>. The demixing pressures were reproducible to within 0.4 MPa.

## RESULTS AND DISCUSSION

### Demixing pressures and modelling of phase boundaries

Figure 2 shows the demixing pressures for the 5 wt% solutions of PDMS in carbon dioxide. The solid lines are the predictions by the Sanchez-Lacombe model. The minimum pressure required for complete miscibility shows great sensitivity to temperature. Initially, the demixing pressures show a large decrease with increasing temperature, but as temperature is further increased, the trend is reversed and the demixing pressures increase with temperature. Thus, the system has characteristics of systems showing both upper and lower critical solution temperatures (*UCST* and *LCST*). This type of behaviour, i.e. merging of the phase boundaries at low temperature (*UCST*) and at high temperature (*LCST*), is not unusual for binary mixtures with a high degree of molecular asymmetry. Such demixing curves have been reported for other polymer-solvent systems such as ethylene-propylene copolymers in propylene<sup>18,19</sup>. The one-phase regions are bounded by the upper portions of each curve. The temperature range where the behaviour shifts from *UCST* to *LCST* is higher than the critical temperature of CO<sub>2</sub> ( $T_c = 304.1$  K and  $P_c = 7.2$  MPa) and is observed to shift to higher temperatures with increasing molecular weight.

It is interesting to note that the demixing pressures for the two high-molecular-weight samples ( $M_w = 369\,200$  and  $273\,500$ ) are very close to each other. We have recently reported on similar behaviour for polyethylene/n-alkane systems<sup>20</sup>, where the demixing pressures of a polyethylene sample of  $M_w = 121\,000$  with a polydispersity index of 4.43 were found to be very close to the demixing pressures of a polyethylene sample of much higher molecular weight  $M_w = 420\,000$  and polydispersity of 2.66. This was shown to be linked to the presence of high-molecular-weight fractions (with molecular weight  $\sim 400\,000$ ) in the sample with high polydispersity even though it had a lower average molecular weight.

For the PDMS samples, the polydispersities are 2.19 ( $M_w = 369\,000$ ) and 2.29 ( $M_w = 273\,500$ ) and thus close to each other. The similarity of the demixing pressures suggests that the lower molecular weight sample must still contain high-molecular-weight fractions that would be comparable to the high-molecular-weight fractions of the higher molecular weight sample. Figure 3 shows the results from gel permeation chromatographic (g.p.c.) analysis of all the PDMS samples. Elution times indicate that the two high-molecular-weight samples indeed have great similarity with respect to their high-molecular-weight tails (the incipient elution times appear identical for both samples), but the one with lower average molecular weight contains greater amount of lower molecular weight fractions (as displayed by the elution curve being extended to longer times). The present results once again point to the observation that the high-molecular-weight fractions in a

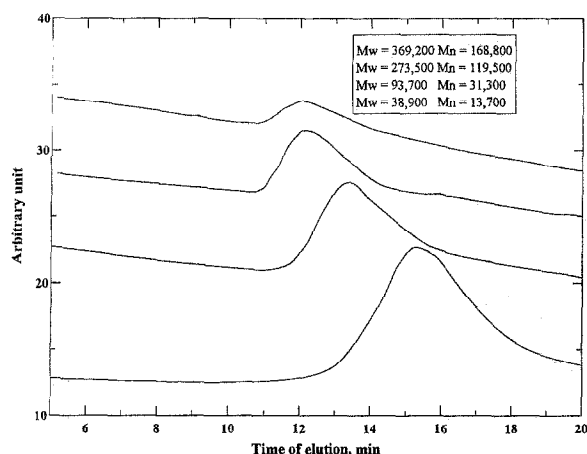


**Figure 3** Analysis of the molecular weight distribution of the poly(dimethylsiloxane) samples by gel permeation chromatography

given polymer influence the demixing pressures which are experimentally observed as cloud points.

Figure 2 also shows the model predictions for the phase boundaries. For these predictions we have used the Sanchez–Lacombe model<sup>21–23</sup>, for which the basic equation of state is given by

$$\tilde{\rho}^2 + \tilde{P} + \tilde{T}[\ln(1 - \tilde{\rho}) + (1 - 1/r)\tilde{\rho}] = 0 \quad (1)$$

where  $\tilde{\rho}$ ,  $\tilde{T}$  and  $\tilde{P}$  are the reduced density ( $\rho/\rho^*$ ), reduced temperature ( $T/T^*$ ) and reduced pressure ( $P/P^*$ ), respectively, and  $r$  represents the number of lattice sites occupied by a molecule. The  $*$  quantities are the characteristic parameters.

The characteristic parameters used in the present calculations are shown in Table 1. The parameters for the polymer were taken directly from the literature<sup>23</sup>. The parameters for the CO<sub>2</sub> were optimized by fitting the *PVT* data in the range 360–420 K and 20–60 MPa using literature *PVT* data<sup>24</sup>. This particular set of literature data was convenient to use since the values reported were obtained in the same temperature and pressure ranges explored in the present study. The characteristic parameters for carbon dioxide have been reported by other workers<sup>11,25</sup> also and are included in Table 1 for comparison. There are differences in the values reported. However, this should not be taken as discrepancy, but rather regarded as an outcome of the fact that they are not necessarily obtained by fitting the same data sets and are optimal only for the specific temperature or pressure range in which they were evaluated. In the modelling of mixtures, the differences in the characteristic parameters may be further masked by the adjustment of the interaction parameter  $\delta_{ij}$  and it is likely that predictions of similar quality can be achieved with any of these parameter sets.

**Table 1** Characteristic parameters for PDMS and CO<sub>2</sub> used in the Sanchez–Lacombe model

Component	$P^*$ (MPa)	$T^*$ (K)	$\rho^*$ (g cm <sup>-3</sup> )	Ref.
PDMS	302.0	476.0	1.104	23
CO <sub>2</sub>	420.0	340.9	1.392	present study
CO <sub>2</sub>	574.5	305.0	1.510	25
CO <sub>2</sub>	464.2	328.1	1.426	11

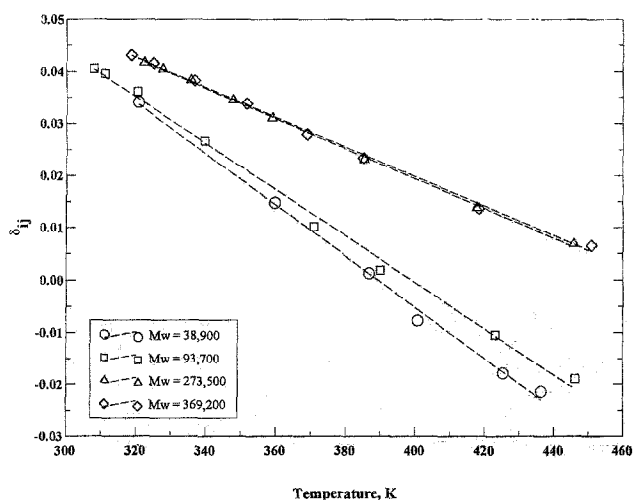


**Figure 4** Temperature dependence of the binary interaction parameter used in the modelling of solutions of poly(dimethylsiloxane) of different molecular weights

The characteristic parameters for the mixture are determined from the pure component values using a set of mixing rules<sup>22</sup> given by the following relationships.

- (a) The characteristic density  $\rho^*$  is related to the hard-core molecular volume  $v^*$  by  $v^* = M/\rho^*$  for both pure substances and the mixtures. For mixtures,  $v^*$  is given by

$$\frac{1}{v^*} = \sum_i \frac{\phi_i}{v_i^*} \quad (2)$$

where  $\phi_i$  represents the close-packed volume fraction and  $v_i^*$  represents the hard-core molecular volume of the  $i$ th component.

- (b) The characteristic pressure  $P^*$  for the mixture is given by the following equation

$$P^* = \sum_j \phi_j P_j^* - RT \sum_j \sum_{i < j} \phi_i \phi_j \chi_{ij} \quad (3)$$

where  $R$  is the gas constant and  $\delta_{ij}$  is the interaction parameter.  $\delta_{ij}$  is given by

$$\frac{\chi_{ij}}{RT} = P_i^* + P_j^* - 2(P_i^* P_j^*)^{1/2}(1 - \delta_{ij}) \quad (4)$$

where the  $P_i^*$  and  $P_j^*$  are the characteristic pressures for the components  $i$  and  $j$ , and  $\delta_{ij}$  is the interaction parameter which is usually a small quantity and corrects for the deviation of the interaction energy from the geometric mean.

**Table 2** Coefficients of the linear equation  $\delta_{ij} = A + BT$  for the temperature dependence of the interaction parameter used in the Sanchez–Lacombe model

Polymer molecular weight ( $M_w$ )	$A$	$B$
38 900	0.19047	$-4.8914 \times 10^{-4}$
93 700	0.17689	$-4.4335 \times 10^{-4}$
273 500	0.13448	$-2.8774 \times 10^{-4}$
369 200	0.13366	$-2.8463 \times 10^{-4}$

(c) The characteristic temperature is defined as

$$T^* = \frac{P^* v_0}{R} \quad (5)$$

where  $v_0$  is the volume of a lattice site per mol. Further details are discussed in the literature<sup>21–23</sup>.

In the present calculations of the phase boundaries, the interaction parameters  $\delta_{ij}$  were first optimized for individual experimental points. They have been plotted as a function of temperature in Figure 4. As shown in the figure,  $\delta_{ij}$  shows a linear variation with temperature for each molecular weight sample. The coefficients of the linear regression equations ( $\delta_{ij} = A + BT$ ) are shown in Table 2. We used the values of  $\delta_{ij}$  as expressed by these linear relationships in the phase boundary calculations. As shown in Figure 2, the calculations using these correlations for the interaction parameters match the experimental data well.

In Figure 4, the interaction parameter  $\delta_{ij}$  is observed to decrease with temperature. An opposite trend was reported by Garg *et al.*<sup>11</sup> who also have used the Sanchez–Lacombe model to predict the solubility of carbon dioxide in PDMS melts. It should be noted that the absolute values of  $\delta_{ij}$  in the present study are much smaller, indicating that only slight adjustments are required with the present set of characteristic parameters. The opposite trend in the temperature dependence of the interaction parameter is not likely to be arising from using different sets of characteristic parameters for CO<sub>2</sub>, it is likely to arise from the differences in concentrations. The present data sets and modelling are for relatively dilute solutions of PDMS in carbon dioxide, whereas the literature values correspond to modelling work conducted at the other extreme corresponding to the solubility of carbon dioxide in PDMS melts.

In addition to the temperature dependence, the fitted values of the interaction parameter  $\delta_{ij}$  have an apparent dependence on the molecular weight of the polymer. Such dependence was also observed in the modelling of polyethylene/*n*-alkane systems<sup>14,15</sup>. Without any temperature and molecular weight adjustments

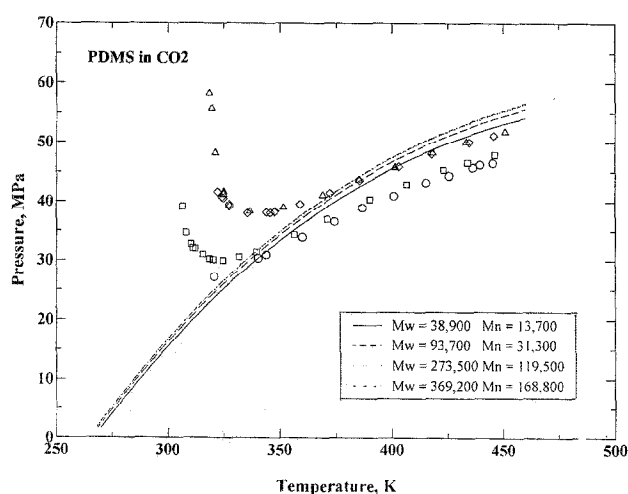


**Figure 5** Experimental demixing pressures for solutions of poly-(dimethylsiloxane) in carbon dioxide, and predictions by the Sanchez–Lacombe model with a fixed value of the interaction parameter,  $\delta_{ij} = 0.0255$

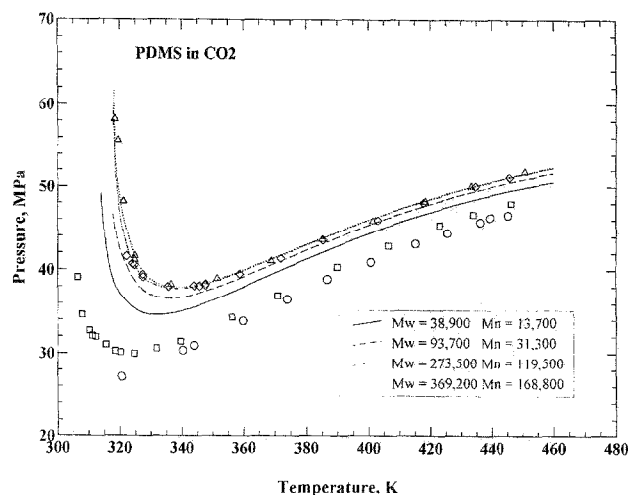


**Figure 6** Experimental demixing pressures for solutions of poly-(dimethylsiloxane) in carbon dioxide, and predictions by the Sanchez–Lacombe model using temperature-dependent interaction parameter for the high-molecular-weight ( $M_w = 369\,200$ ) polymer sample [ $\delta_{ij} = 0.13366 - 2.8463 \times 10^{-4}T$ ]

to the interaction parameter, the predictive power of the Sanchez–Lacombe model is limited. Figure 5 shows the model predictions if a fixed value of the interaction parameter is used. Here  $\delta_{ij}$  is taken to be 0.0255 (the value for the  $M_w = 369\,200$  samples at 380 K). At low temperatures, the shift from *LSCT* to *UCST* is not predicted. At higher temperatures, the qualitative trends with molecular weight are predicted but the match with experimental data is poor. Figure 6 shows the model predictions if the temperature-dependent interaction parameters determined for the sample with  $M_w = 369\,200$  are used. The general trend of the phase boundary is predicted over the whole temperature range for all molecular weights, but the quantitative agreement with experimental data for the lower molecular weight samples is not achieved. If, instead, the temperature-dependent interaction parameter for

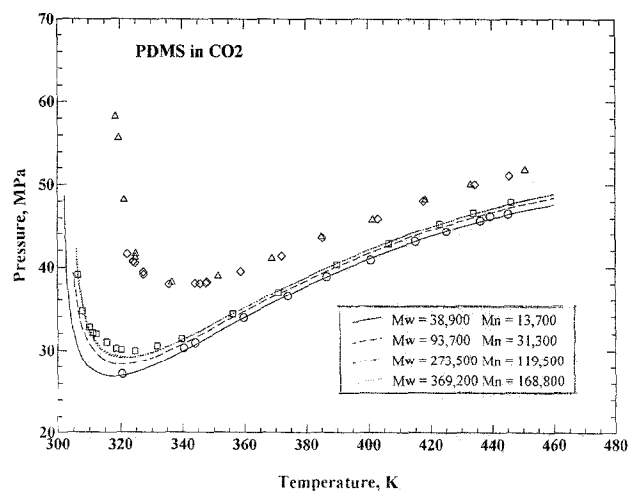


**Figure 7** Experimental demixing pressures for solutions of poly-(dimethylsiloxane) in carbon dioxide, and predictions by the Sanchez–Lacombe model using temperature-dependent interaction parameter for the low-molecular-weight ( $M_w = 38\,900$ ) polymer sample [ $\delta_{ij} = 0.19047 - 4.8914 \times 10^{-4}T$ ]

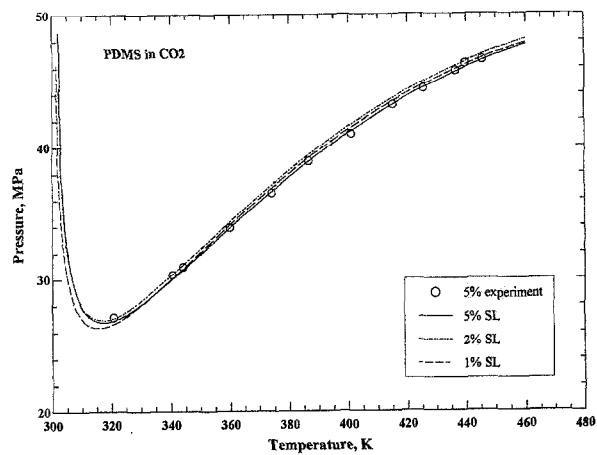


**Figure 8** Demixing pressures of solutions of poly(dimethylsiloxane) ( $M_w = 38\,900$ ) in supercritical carbon dioxide at 1, 2 and 5 wt% concentrations. Solid lines are the model predictions. Data represents the 5 wt% solution

the lower molecular weight sample ( $M_w = 38\,900$ ) is used in the predictions, the results show deviations for the higher molecular weight samples. This is shown in Figure 7.

As shown in Figure 2, if temperature- and molecular-weight-dependent interaction parameters are used, experimental data can be represented well. Previous work on polyethylene/alkane systems has shown that the concentration dependence can also be represented well when using such parameters for a given polymer/solvent system. Even though we have not generated extensive experimental data for the concentration dependence with the PDMS/carbon dioxide system, it is expected that the model would give reasonable predictions. Figure 8 shows the experimental data on the demixing pressures for the sample with  $M_w = 38\,900$  at 5 wt% and the predictions using the temperature-dependent interaction parameters for this molecular weight (Table 2, Figure 4) at 1, 2 and 5 wt% concentrations.

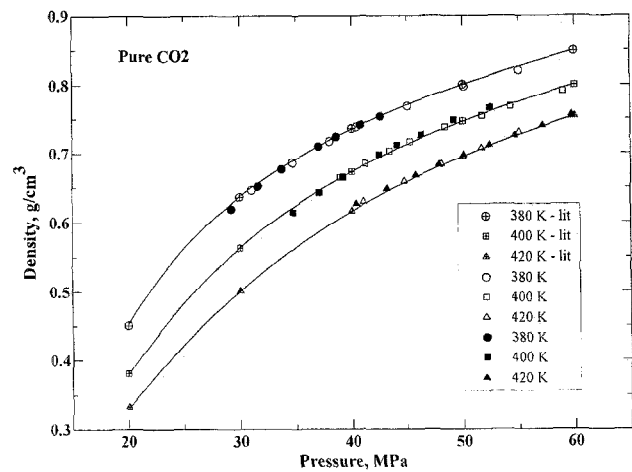


**Figure 9** Pressure dependence of the density of pure carbon dioxide at selected temperatures. Solid lines are predictions by the Sanchez-Lacombe model

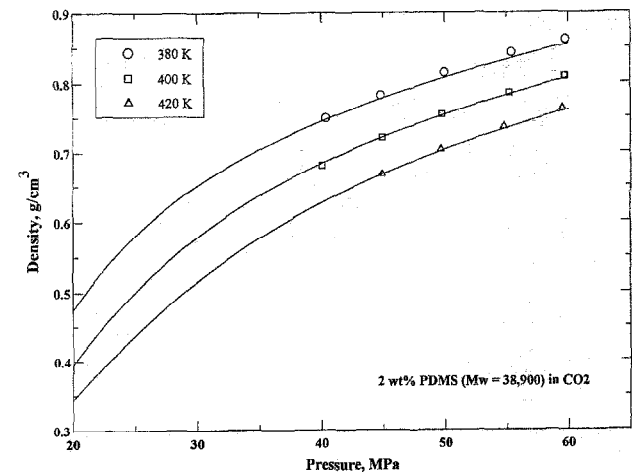


**Figure 11** Density of the 2 wt% solution of poly(dimethylsiloxane) in supercritical carbon dioxide. Solid lines represent the predictions by the Sanchez-Lacombe model

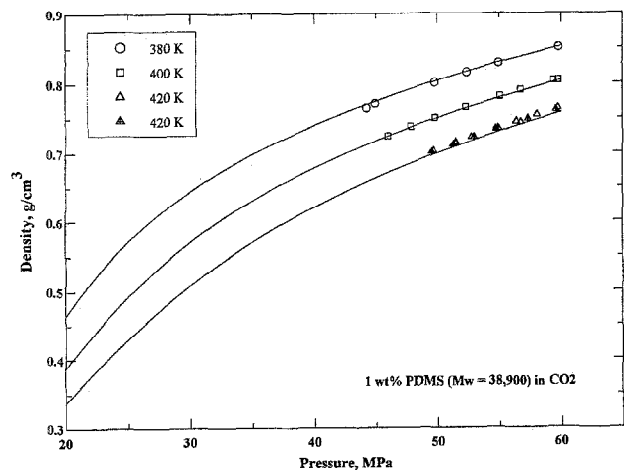


**Figure 10** Density of the 1 wt% solution of poly(dimethylsiloxane) in supercritical carbon dioxide. Solid lines represent the predictions by the Sanchez-Lacombe model

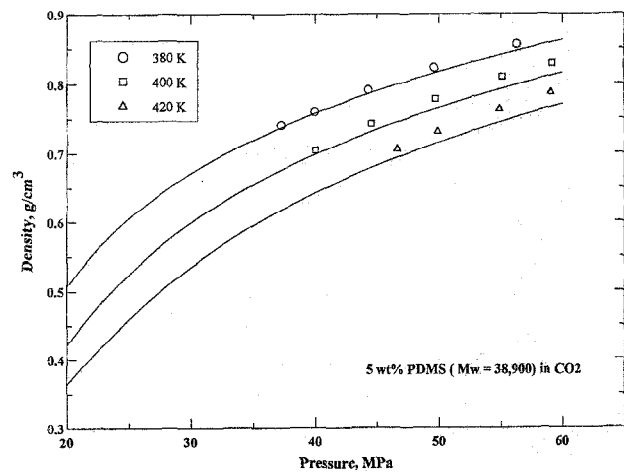


**Figure 12** Density of the 5 wt% solution of poly(dimethylsiloxane) in supercritical carbon dioxide. Solid lines represent the predictions by the Sanchez-Lacombe model

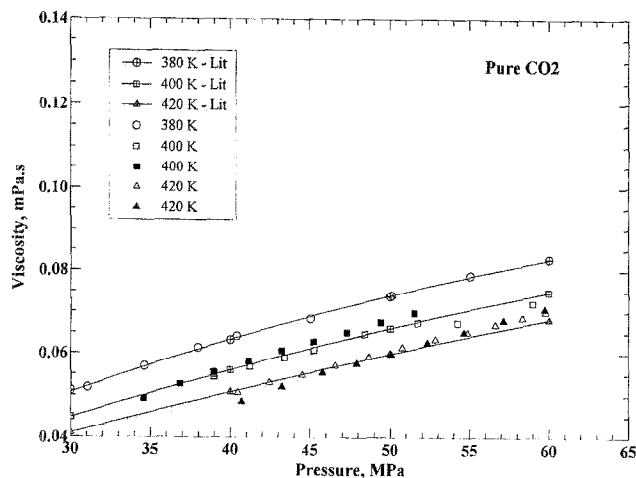


**Figure 13** Variation of viscosity of pure carbon dioxide with pressure. Comparison of experimental data with literature data

### Density

To ensure the reliability of the density measurements, the density of pure carbon dioxide was determined at 380, 400 and 420 K and compared with literature values<sup>24</sup>. The results are shown in Figure 9, where data from repeat runs at different temperatures are included to demonstrate the reproducibility. The agreement is excellent. The solid lines are the predictions by the Sanchez-Lacombe model [equation (1)] using the characteristic parameters given in Table 1.

Figures 10–12 show the density data for 1, 2 and 5 wt% solutions of PDMS ( $M_w = 38\,900$ ) in carbon dioxide at 380, 400 and 420 K in the pressure range from 40 to 70 MPa. In Figure 10, the densities at 420 K from a repeat run have been included to demonstrate the reproducibility of the data for these polymer solutions. The solid lines in the figures are again the predictions by the Sanchez-Lacombe equation of state.

The experimental values in these figures have been obtained at temperatures and pressures corresponding to homogeneous one-phase regions. The phase behaviour at low temperatures shown in Figures 2 and 8 emphasizes the importance of ensuring that the system is in the homogeneous solution phase. Recently, extrapolations of viscosity data from very high polymer concentrations have been used to cover the full concentration range for presentation of parameters such as the activation volume, or flow activation energies<sup>6</sup>. The present observations on phase behaviour reveal that complications stemming from phase separation may arise at low concentrations, especially at low temperatures, and such extrapolations must be used with caution.

It is clear from the comparison of the experimental data and model predictions for density of the solutions, that the Sanchez-Lacombe model is effective in describing not only the phase boundaries but also the general *PVT* behaviour of these solutions.

### Viscosity

Viscosity measurements were conducted at 380, 400 and 420 K for pure carbon dioxide and for solutions of PDMS ( $M_w = 38\,900$ ) in carbon dioxide. Viscosities for the higher molecular weight samples are being determined and will be reported at a later date.

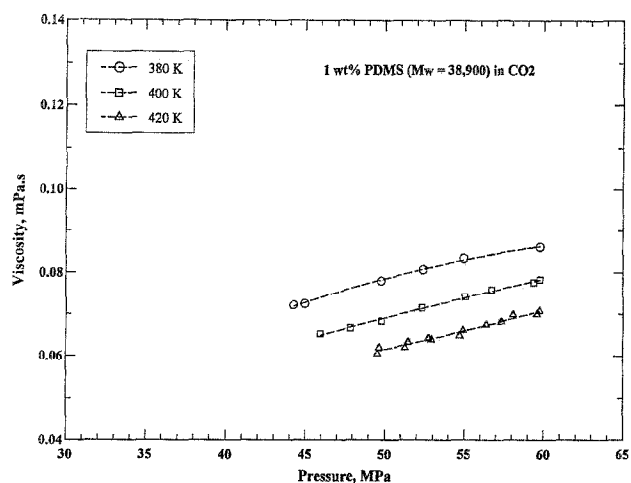


**Figure 14** Variation of viscosity with pressure for poly(dimethylsiloxane) ( $M_w = 38\,900$ ) solutions (1 wt%) in carbon dioxide at different temperatures

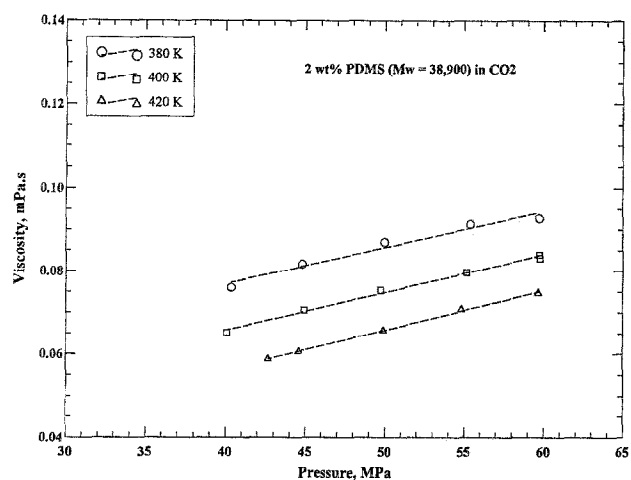


**Figure 15** Variation of viscosity with pressure for poly(dimethylsiloxane) ( $M_w = 38\,900$ ) solutions (2 wt%) in carbon dioxide at different temperatures

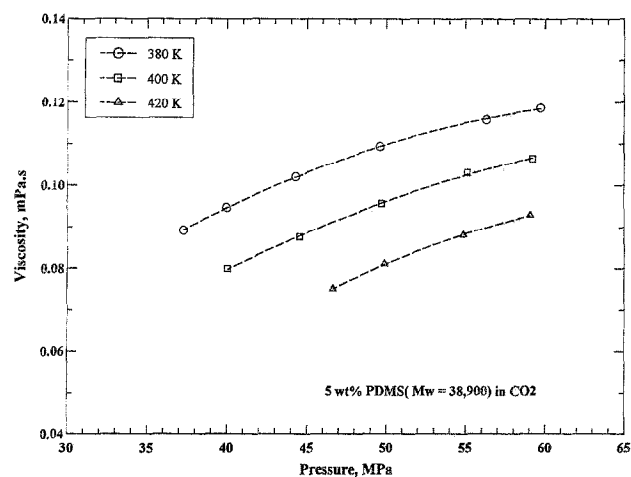


**Figure 16** Variation of viscosity with pressure for poly(dimethylsiloxane) ( $M_w = 38\,900$ ) solutions (5 wt%) in carbon dioxide at different temperatures

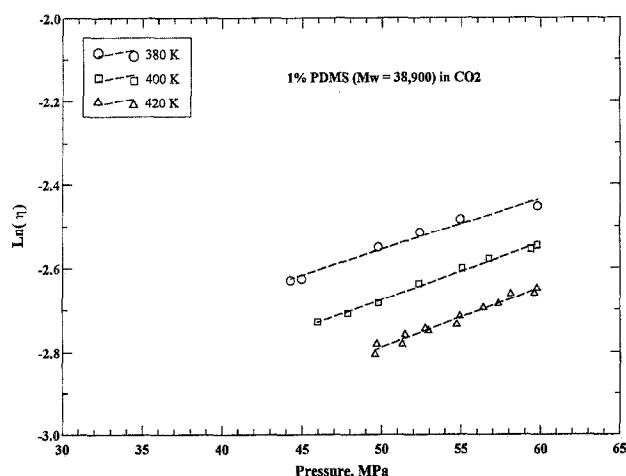


**Figure 17** Variation of  $\ln(\text{viscosity})$  with pressure for poly(dimethylsiloxane) ( $M_w = 38\,900$ ) solutions (1 wt%) in carbon dioxide at different temperatures

**Table 3** Apparent activation volumes  $V^\#$  ( $\text{cm}^3 \text{mol}^{-1}$ ) calculated from  $\partial \ln(\eta)/\partial P|_{T, \text{conc}} = V^\#/RT$  in the pressure range from 40 to 70 MPa

Temperature (K)	Polymer concentration (wt%)		
	1	2	5
380	38.0	32.6	39.2
400	44.8	40.7	49.9
420	49.3	50.1	58.7

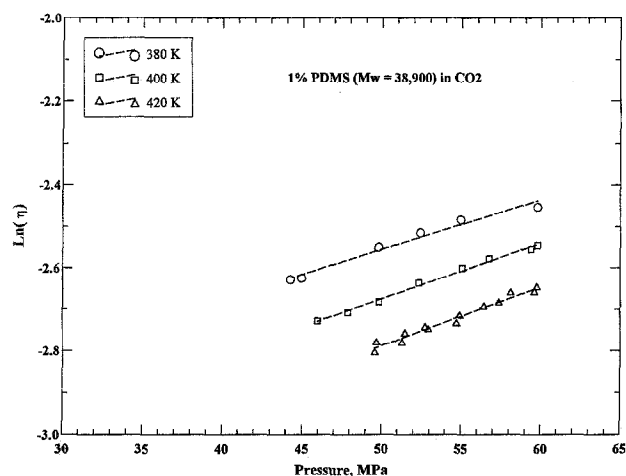


**Figure 18** Variation of  $\ln(\text{viscosity})$  with inverse temperature for poly(dimethylsiloxane) ( $M_w = 38\,900$ ) solutions (1 wt%) in carbon dioxide at different pressures

**Table 4** Flow activation energies  $E$  ( $\text{kJ mol}^{-1}$ ) calculated from  $\partial \ln(\eta)/\partial (1/T)|_{P, \text{conc}} = E/R$  in the temperature range from 380 to 420 K

Pressure (MPa)	Polymer concentration (wt %)		
	1	2	5
45	7.0	7.4	8.1
50	7.4	8.1	8.8
55	7.7	8.8	9.5
60	8.0	9.5	10.3

Figure 13 shows the variation of viscosity of pure carbon dioxide with pressure at each temperature, the present data being compared with the literature values. Literature data<sup>26</sup> for the viscosity of carbon dioxide at 380 K were used in calibration of the viscometer for these low viscosity fluids and therefore they exactly match. At 400 and 420 K, data from repeat experiments have been included. As shown in the figure, the experimental values are in good agreement with the literature at these two temperatures.

Viscosity data for the PDMS solutions (1, 2 and 5% by weight) are shown in Figures 14–16. The general trends in these figures are as expected, i.e. viscosity increases with pressure, decreases with temperature, and increases with the concentration of polymer.

**Pressure dependence of viscosity.** Pressure dependence of viscosity is often discussed in terms of the activation volume in accordance with the following relationships

$$\eta = A \exp\left(\frac{V^\# P}{RT}\right) \quad (6)$$

or

$$\left.\frac{\partial \ln(\eta)}{\partial P}\right|_{T, \text{conc}} = \frac{V^\#}{RT} \quad (7)$$

where  $\eta$  is the viscosity,  $V^\#$  is the volume of activation,  $R$  is the gas constant,  $P$  is the pressure,  $T$  is the temperature and  $A$  is a prefactor. The viscosity data presented in Figures 14–16 have been analysed according to these relationships. As an example, Figure 17 shows the variation of  $\ln(\eta)$  with pressure for the 1 wt% polymer solution at the designated temperatures. From the slopes at the respective temperatures, the activation volumes have been calculated. The results are shown in Table 3 for all concentrations (i.e. 1, 2 and 5% by weight). The activation volumes were observed to increase with both temperature and concentration, the effect of concentration however being less significant at these low concentrations. In going from 380 to 420 K, the activation volume increased from  $\sim 30$  to  $60 \text{ cm}^3 \text{mol}^{-1}$ . Mertsch and Wolf<sup>6</sup> recently reported activation volumes in the range of  $10\text{--}40 \text{ cm}^3 \text{mol}^{-1}$  for PDMS ( $M_w = 74\,000$ )/CO<sub>2</sub> mixtures for the entire concentration range at low temperatures (303 K). (The data for the solutions with concentrations  $< 25\%$  volume fraction were extrapolated from the data for high concentration solutions by those authors. As indicated earlier, extrapolation of data to low temperatures must be viewed with caution since two-phase regions may be entered if pressures are not sufficiently high. Nonetheless, considering the higher temperatures explored in the present study, these results appear consistent with each other.) At temperatures comparable to those in the present study, for high-pressure solutions of polyethylenes in *n*-pentane, activation volumes are in the range  $30\text{--}45 \text{ cm}^3 \text{mol}^{-1}$  (ref. 7).

**Temperature dependence of viscosity.** The temperature dependence of viscosity for polymer solutions is traditionally described by Arrhenius-type relationships, i.e.

$$\eta = A \exp\left(\frac{E}{RT}\right) \quad (8)$$



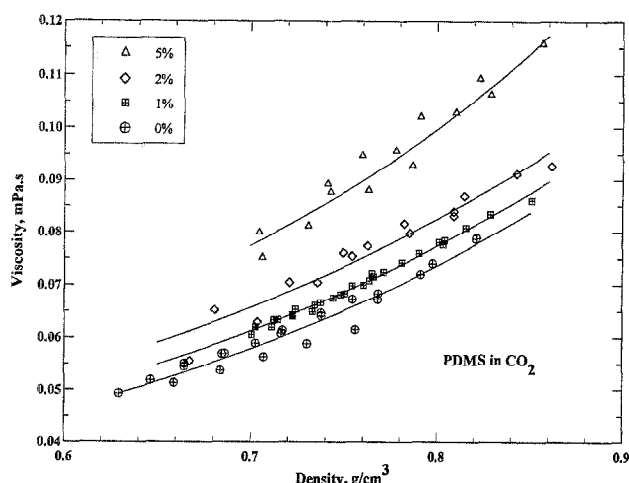


**Figure 19** Variation of viscosity with density for pure carbon dioxide and for poly(dimethylsiloxane) ( $M_w = 38\,900$ ) solutions (1, 2 and 5 wt%) in carbon dioxide. Solid lines are the correlations based on free-volume relationships

or

$$\left. \frac{\partial \ln(\eta)}{\partial (1/T)} \right|_{P, \text{conc}} = \frac{E}{R} \quad (9)$$

where  $E$  is the flow activation energy,  $R$  is the gas constant and  $T$  is the temperature. Using the data shown in Figures 14–16,  $\ln(\eta)$  versus  $1/T$  plots have been generated and activation energies have been calculated. Figure 18 shows the results for the 1 wt% solution of PDMS at selected pressures. The activation energies given in Table 4, are in the range 7–10 kJ mol<sup>−1</sup> and are consistent with the literature values<sup>6</sup> for PDMS solutions in CO<sub>2</sub> at similar polymer concentrations. For 1 wt% solutions of polyethylene in n-pentane at high pressures, flow activation energies of 8–12 kJ mol<sup>−1</sup> have been reported<sup>7</sup>.

**Density dependence of viscosity.** In our previous publications<sup>4,7,12</sup> density was used quite successfully as a scaling factor for the viscosity of pure fluids and polymer solutions. Recent comparisons of different relationships have shown that the Doolittle-type free-volume based relationship, in particular

$$\eta = A \exp\left(\frac{B}{1 - V_0\rho}\right) \quad (10)$$

where  $B$  is constant,  $\rho$  is density and  $V_0$  is close-packed volume, is effective in describing polymer solutions<sup>7</sup>.

**Table 5** Coefficients of the equation  $\eta = A \exp[B/(1 - C\rho)]$  for the density dependence of viscosity of PDMS ( $M_w = 38\,900$ ) solutions in CO<sub>2</sub>

Polymer concentration (wt%)	$A$	$B$	$C (= V_0)$	$SE^a$
0 (pure CO <sub>2</sub> )	$1.118 \times 10^{-4}$	4.9544	0.296	$1.74 \times 10^{-3}$
1	$1.226 \times 10^{-4}$	4.9559	0.289	$6.00 \times 10^{-4}$
2	$1.338 \times 10^{-4}$	4.9641	0.284	$2.506 \times 10^{-3}$
5	$1.430 \times 10^{-4}$	4.9481	0.305	$3.022 \times 10^{-3}$

<sup>a</sup> Standard error of estimating the viscosities using the given coefficients;  $SE = \{\sum[y_i - y_{cal,i}]^2/n\}^{1/2}$ , where  $y_i$  and  $y_{cal,i}$  are the experimental and the calculated values, and  $n$  is the number of data points

Here, the free-volume fraction  $V_f = (1 - V_0\rho)$  or  $(V - V_0)/V$  considers the free volume at the prevailing conditions (i.e. at the conditions corresponding to the actual solution volume  $V$ ). This relationship has been used to correlate the viscosity data obtained in the present study also. The results are shown in Figure 19, where the solid lines represent equation (10). As shown, the data at different temperatures and pressures merge into one curve in the density domain and are well described by equation (10). The parameters for the relationships are given in Table 5, where it can be seen that a value of 0.29 cm<sup>3</sup> g<sup>−1</sup> is suggested for the close-packed volume for carbon dioxide and remains essentially unchanged for these dilute solutions. A value of 0.44 cm<sup>3</sup> g<sup>−1</sup> is reported for the van der Waals' volume for carbon dioxide<sup>25</sup> and a value of 0.346 cm<sup>3</sup> g<sup>−1</sup> is calculated from the Carnahan–Starling van der Waals' equation of state<sup>26</sup>. Similar analysis of viscosity data for solutions of polyethylene and n-pentane suggests<sup>7</sup> a  $V_0$  value of 0.42 cm<sup>3</sup> g<sup>−1</sup>. For n-pentane, the van der Waals' volume is 0.8 cm<sup>3</sup> g<sup>−1</sup> (ref. 25) and the hard-sphere volume calculated from the Carnahan–Starling van der Waals' equation of state is 0.75 cm<sup>3</sup> g<sup>−1</sup>. It is interesting to note that, even though the occupied volumes for these solvents predicted from the present viscosity data are numerically smaller, the ratio ( $r$ ) of the predicted value of the close-packed volume of pentane to carbon dioxide ( $r = 1.45$ ) is similar to the ratio calculated from the van der Waals' ( $r = 1.82$ ) or the Carnahan–Starling equation of state ( $r = 2.16$ ).

## CONCLUSIONS

This study has shown that the densities and the phase behaviour of solutions of poly(dimethylsiloxane)s in supercritical carbon dioxide can be described well with the Sanchez–Lacombe model. It is shown that the molecular weight and molecular weight distributions have a significant effect on the observed demixing pressures. Viscosities of these solutions show the usual behaviour in that temperature dependence follows Arrhenius-type behaviour with flow activation energies of about 8 kJ mol<sup>−1</sup>. Pressure dependence is also exponential, with the apparent volume of activation being in the range of 30–60 cm<sup>3</sup> mol<sup>−1</sup>. The effect of temperature and pressure are unified with density and the viscosity data are best correlated with Doolittle-type free-volume based relationships of the form  $\eta = A \exp[B/(1 - V_0\rho)]$ .

## ACKNOWLEDGEMENT

The research has been supported in part by funding from the USDA (Grant 92-37103-7989).

## REFERENCES

- 1 Kiran, E. in 'Supercritical Fluids. Fundamentals for Application', (Eds E. Kiran and J. M. H. Levelt Sengers), Kluwer Academic Publishers, Dordrecht, 1994
- 2 Bair, S. and Winter, W. D. *Tribol. Trans.* 1993, **36**(4), 721
- 3 Heller, J. P. and Dandge, D. K. Paper presented at Int. Symp. on Oil-field and Geothermal Chemistry, Denver, CO, 1–3 June 1983
- 4 Kiran, E. and Sen, Y. L. in 'Supercritical Fluid Engineering

- Science' (Eds E. Kiran and J. F. Brennecke), ACS Symposium Series 514, American Chemical Society, Washington, DC, 1993, p. 104
- 5 Gerhard, L. J., Garg, A., Manke, C. and Gulari, E. in 'Proc. 3rd Int. Symp. on Supercritical Fluids', Strasbourg, France, 17–19 October 1994, Vol. 3, p. 265
- 6 Mertch, R. and Wolf, B. A. *Macromolecules* 1994, **27**, 3289
- 7 Kiran, E. and Gokmenoglu, Z. *J. Appl. Polym. Sci.* in press
- 8 Yilgor, I., McGrath, J. E and Krukoni, V. J. *Polym. Bull* 1984, **12**, 499
- 9 McHugh, M. A. and Krukoni, V. J. 'Supercritical Fluid Extraction', 2nd Edn, Butterworth, Boston, MA, 1994
- 10 Krishnamurthy, S. and Chen, S. H. *Makromol. Chem.* 1989, **190**, 1407
- 11 Garg, A., Gulari, E. and Manke, C. W. *Macromolecules* 1994, **27**, 5643
- 12 Kiran, E. and Sen, Y. L. *Int. J. Thermophys.* 1992, **13**, 411
- 13 Sen, Y. L. and Kiran, E. *J. Supercrit. Fluids* 1990, **3**(2), 91
- 14 Kiran, E., Xiong, Y. and Zhuang, W. *J. Supercrit. Fluids* 1993, **6**, 193
- 15 Xiong, Y. and Kiran, E. *Polymer* 1994, **35**, 4408
- 16 Xiong, Y. and Kiran, E. in 'Proc. 3rd Int. Symp. on Supercritical Fluids', Strasbourg, France, 17–19 October 1994, Vol. 3, p. 271
- 17 Xiong, Y. and Kiran, E. *J. Appl. Polym. Sci.* 1995, **55**, 1805
- 18 Chen, S. J. and Radosz, M. in 'Proc. 2nd Int. Symp. on Supercritical Fluids', Boston, MA, 10–12 May 1991, p. 225
- 19 Chen, S. J., Economou, I. G. and Radosz, M. *Macromolecules* 1992, **25**, 4987
- 20 Kiran, E., Xiong, Y. and Zhuang, W. *J. Supercrit. Fluids* 1994, **7**, 283
- 21 Sanchez, I. C. and Lacombe, R. H. *J. Phys. Chem.* 1976, **80**, 2352
- 22 Lacombe, R. H. and Sanchez, I. C. *J. Phys. Chem.* 1976, **80**, 2568
- 23 Sanchez, I. C. and Lacombe, R. H. *Macromolecules* 1978, **11**, 1145
- 24 Vargaftik, N. B. 'Tables on the Thermophysical Properties of Liquids and Gases', 2nd Edn, John Wiley & Sons, New York, 1975
- 25 Kiszka, M. B., Meilchen, M. A. and McHugh, M. A. *J. Appl. Polym. Sci.* 1988, **36**, 583
- 26 Stephan, K. and Lucas, K. 'Viscosity of Dense Fluids', Plenum Press, New York, 1979
- 27 Bondi, A. *J. Phys. Chem.* 1964, **68**(3), 441
- 28 Arnotz, D. B. and Herschbach, D. R. *J. Phys. Chem.* 1990, **94**, 1038